Adapting an MSE controller for active noise control to nonstationary noise statistics

Annea BARKEFORS[1]; Mikael STERNAD[2]

[1] Uppsala University and Dirac Research AB, Sweden

[2] Uppsala University and Dirac Research AB, Sweden

ABSTRACT

In feedforward active noise control, a primary noise signal is used to generate control signals via a set of loudspeakers. In problems where many loudspeakers are used, it becomes difficult to adjust the controller filters to fast changing spectral properties of broadband primary noise signals. Many parameters then need to be readjusted simultaneously, which limits the tracking performance of e.g. filtered-x LMS adaptation algorithms. Here we propose and evaluate two feedforward control methods based on linear quadratic gaussian control that adapt to the often time-varying statistical properties of the feedforward noise signal, in a partly indirect adaptive design. For both proposed methods, the time is divided in batches and the control laws are updated for each time batch based on repeated estimates of the noise statistics. In the first method, the estimates of the noise statistics are incorporated into the controller, which is updated for each batch, whereas in the second method the controller is kept constant and a predictor for the noise is updated. The first method seems promising, and shows a gain in attenuation of about 5 dB over a controller that disregards the feedforward noise statistics. The second method, however, shows no such advantage.

Keywords: Active Noise Control, Feedforward, Adaptive I-INCE Classification of Subjects Number(s): 38.2

1. INTRODUCTION

Low frequency noise is difficult to attenuate by passive means. As a lucky coincidence, it is for lower frequencies that Active Noise Control (ANC) works best. In ANC, the sound field of the undesired noise is matched with a sound field with opposite phase by the use of secondary loudspeakers. Destructive interference between the two soundfields then creates a zone in which the undesired noise is attenuated. Possible applications for ANC include car compartments, where local zones of attenuation of road noise or engine noise can be created around the heads of driver and passengers. Here, we look at the possibility to attenuate simulated engine noise around the head of a passenger. We use a polynomial approach to calculate a Linear Quadratic Gaussian (LQG) Mean Square Error (MSE) controller. Previously in our work (1, 2) we have assumed that all transfer functions are time-invariant. Our modeling and design has therefore been done offline and the resulting controller has never been updated. However, this assumption is often incorrect. There are for example many situations when the noise source is of a varying nature. In the example of a car compartment, most of the noise sources cannot be modeled as stationary AR models. Engine noise will vary depending on the engine speed (rpm value) and road noise will vary depending on the speed of the vehicle and the structure of the road. One way around this is to use purely adaptive methods, as is the approach of many researchers today (3, 4, 5, 6). Another is to leave out the statistics of the noise source in the controller design, resulting in a controller that only takes into account the noise paths from the measurable disturbances and the control paths. Here we propose and evaluate two methods that do take time-varying statistical properties of the feedforward signal into account but in which only a part of the system is adaptive. The basis of the methods are the design equations for LQG feedforward controller design as outlined in Section 2.1. However, an estimate of the AR noise model is updated and replaced periodically.

[1] annea.barkefors@signal.uu.se

[2] mikael.sternad@signal.uu.se

1.1 Mathematical notation

Vectors are here represented by bold lowercase letters, such as $\mathbf{v}(t)$, and scalars are written in italics. Matrices of causal FIR filters are represented in the time domain by matrices $\boldsymbol{P}(q^{-1})$ of polynomials in the backward shift operator q^{-1}, where $q^{-1}\mathbf{v}(t) = \mathbf{v}(t-1)$. The time-domain operator q^{-1} corresponds to z^{-1} or $e^{-j\omega}$ in the frequency domain. The transpose of a matrix $\mathbf{M}$ is denoted $\mathbf{M}'$. For a polynomial matrix $\boldsymbol{P}(q^{-1})$, the corresponding conjugate matrix $\boldsymbol{P}_*(q)$ is defined as its conjugate transpose, with the forward shift operator q substituted for q^{-1}. Rational matrices $\mathcal{R}(q^{-1})$ of IIR filters will be represented by uppercase calligraphic symbols. Arguments are omitted below where there is no risk of misunderstanding.

2. THE ACOUSTIC SYSTEM

We consider an acoustic system consisting of N control loudspeakers and M measurement positions covering an area or volume to be controlled. The transfer functions between the $N \times 1$ input vector $\mathbf{u}(t)$ and the $M \times 1$ output vector $\mathbf{y}(t)$ is modeled as an $M \times N$ polynomial matrix of FIR filters

$$\mathbf{y}(t) = \boldsymbol{B}(q^{-1})\mathbf{u}(t)\ . \tag{1}$$

A second $M \times L$ polynomial matrix of FIR filters

$$\mathbf{z}(t) = \boldsymbol{D}(q^{-1})\mathbf{n}(t) \tag{2}$$

is modeled to describe the noise paths from the $L \times 1$ vector of measurable disturbances, or feedforward signals, $\mathbf{n}(t)$ to the M measurement positions. Furthermore, the measurable disturbance is modeled as a vector-AR process

$$\mathbf{n}(t) = \boldsymbol{F}^{-1}(q^{-1})\mathbf{e}(t)\ , \tag{3}$$

where $\boldsymbol{F}(q^{-1})$ is assumed diagonal and $\mathbf{e}(t)$ is an $L \times 1$ vector of white noise with covariance matrix $E(\mathbf{e}(t)\mathbf{e}^T(t)) = \Lambda_e$. For this system a linear feedforward controller is to be designed to achieve ANC in the region spanned by the M control points. We do not assume online measurements of the sound in any of these points when the controller is operating.

2.1 Optimal controller design

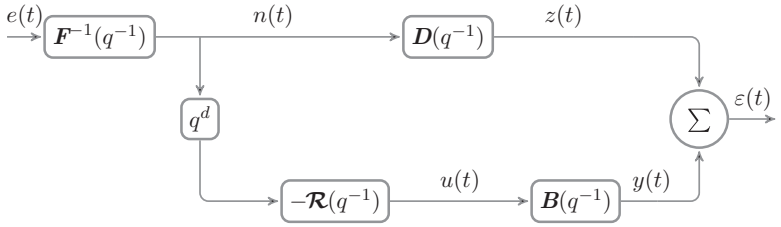

Figure 1 – Block diagram for the system setup in the controller design.

As the block diagram in Figure 1 shows, the controller to be designed acts on the feedforward signal shifted d samples forward in time:

$$\mathbf{u}(t) = -\mathcal{R}(q^{-1})\mathbf{n}(t+d)\ . \tag{4}$$

The time advance d is a modeling parameter which can be used when the disturbance signal is predictable. This controller will give rise to the remaining error after control

$$\boldsymbol{\varepsilon}(t) = (q^{-d}\boldsymbol{D} - \boldsymbol{B}\mathcal{R})\mathbf{n}(t+d)\ , \tag{5}$$

which is to be minimized using the scalar quadratic criterion that represents the control-weighted MSE

$$J = E\{(\boldsymbol{V}\boldsymbol{\varepsilon}(t))'\boldsymbol{V}\boldsymbol{\varepsilon}(t) + (\boldsymbol{W}\mathbf{u}(t))'\boldsymbol{W}\mathbf{u}(t)\}\ , \tag{6}$$

under constraints of stability and causality of the controller $\mathcal{R}(q^{-1})$. In the criterion, the $M \times M$ control error penalty matrix $\boldsymbol{V}(q^{-1})$ can be used to introduce different weights on the control errors in different measurement positions, frequency regions or signal subspaces. The $N \times N$ control signal penalty matrix $\boldsymbol{W}(q^{-1})$ can be used similarly, as discussed in more detail in (7).

It is shown in Section 3.3 of (8) that under the assumption that $\boldsymbol{W}_*(z)\boldsymbol{W}(z^{-1})$ is positive definite on the unit circle $|z| = 1$, the optimal controller for the system equations (1), (2), (3) with respect to the criterion (6) is given by

$$\mathcal{R} = \boldsymbol{\beta}^{-1}\boldsymbol{Q}\,, \tag{7}$$

where the $N \times N$ polynomial matrix $\boldsymbol{\beta}(q^{-1})$ is the polynomial spectral factor defined by

$$\boldsymbol{\beta}_*\boldsymbol{\beta} = \boldsymbol{B}_*\boldsymbol{V}_*\boldsymbol{V}\boldsymbol{B} + \boldsymbol{W}_*\boldsymbol{W}\,, \tag{8}$$

and the $N \times L$ polynomial matrix $\boldsymbol{Q}(q^{-1})$, together with the $N \times L$ polynomial matrix $\boldsymbol{L}_*(q)$, is the solution to the polynomial matrix Diophantine equation

$$q^{-d}\boldsymbol{B}_*\boldsymbol{V}_*\boldsymbol{V}\boldsymbol{D} = \boldsymbol{\beta}_*\boldsymbol{Q} + q\boldsymbol{L}_*\boldsymbol{F}\,. \tag{9}$$

For a deeper analysis of the controller and its design parameters d and $\boldsymbol{W}(q^{-1})$, particularly for use in ANC, see (7, 9).

3. ADAPTATION TO NONSTATIONARY NOISE STATISTICS

Here we propose two methods for incorporating adaptation with respect to a time-varying noise model $\boldsymbol{F}(q^{-1})$ in eq. (3). An estimate of the model is updated and replaced regularly. This is not needed every sample but can be done at a slower pace if the noise statistics change slowly compared to the sampling frequency. The time is thus in the following divided into batches with the controller kept constant within each batch.

3.1 The noise statistics

The statistics of the measurable feedforward noise signal is assumed to be described by a time-varying AR model

$$\mathbf{n}(t) = \boldsymbol{F}^{-1}(q^{-1},t)\mathbf{e}(t)\,, \tag{10}$$

where $\boldsymbol{F}$ has dimensions $L \times L$ and $\mathbf{e}(t)$ is an $L \times 1$ vector containing white noise with covariance matrix Λ_e. This covariance matrix may be time-varying, but it need not be estimated since it plays no role in the design equations (7), (8), (9). In the evaluation performed in this work, the model (10) is scalar ($L = 1$) and is designed to describe and track the frequencies corresponding to the first two engine orders of a four-cylinder engine by placing complex-conjugated pole pairs close to the unit circle, with radius 0.99, at the corresponding frequencies

$$\omega_n = 2n * \frac{\text{rpm}}{60} * 2\pi\,, \tag{11}$$

giving rise to a fourth order polynomial $\boldsymbol{F}(q^{-1},t) = 1 + f_1(t)q^{-1} + f_2(t)q^{-2} + f_3(t)q^{-3} + f_4(t)q^{-4}$. The angles of these poles are then continuously moved over time to simulate changes in rpm.

The autoregressive system (10) will be modeled online for each time batch, leading to a sequence of AR models. The use of AR models for the noise statistics instead of ARMA models is because AR models have nicer properties, an example of which are the tracking properties which are important for our application but are much worse for ARMA models.

3.2 Method 1

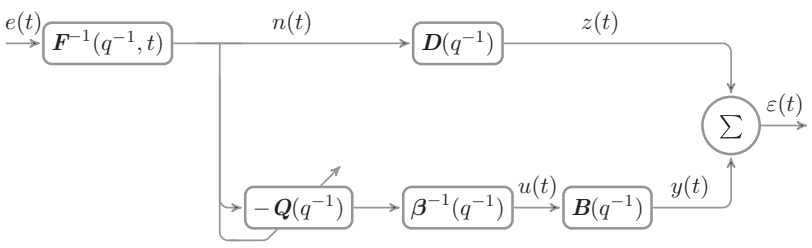

Figure 2 – Block diagram describing the division of the controller block $\mathcal{R}(q^{-1})$ in Figure 1 into one adaptive block $\boldsymbol{Q}(q^{-1})$ and one nonadaptive block $\boldsymbol{\beta}^{-1}(q^{-1})$ in *Method 1*.

In the first proposed method, which will be referred to in the following simply as *Method 1*, the controller $\mathcal{R}(q^{-1})$ in (7) is partitioned into its constituent factors $\boldsymbol{Q}(q^{-1})$ and $\boldsymbol{\beta}^{-1}(q^{-1})$ as illustrated in the block diagram in Figure 2. The spectral factorization (8) does not contain $\boldsymbol{F}$ and $\boldsymbol{\beta}(q^{-1})$ can thus be calculated

offline. Furthermore, the solution of the diophantine equation (9) can to a large extent be prepared in advance, since $\boldsymbol{F}$ is present only in the last term.

During simulation, the simulated time is divided into batches and for each time batch, an estimate $\hat{\boldsymbol{F}}(q^{-1})$ of $\boldsymbol{F}(q^{-1},t)$ is calculated based on the noise signal $n(t)$ in the previous time batch, using the covariance method[1]. The estimate $\hat{\boldsymbol{F}}(q^{-1})$, together with $d = 0$, are used in the Diophantine equation which is solved and the coefficients of $\boldsymbol{Q}(q^{-1})$ are replaced with their updated values in the simulation.

The computational burden is significant for this method since it involves repeated solutions of the Diophantine equation (9). However, if successfully implemented, it has the potential to provide very good performance due to the incorporation of the current noise statistics into the controller design.

3.3 Method 2

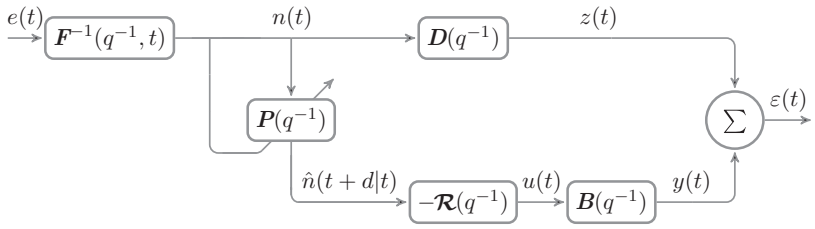

Figure 3 – Block diagram describing *Method 2* with the time advance block q^d in Figure 1 replaced with an adaptive predictor $\boldsymbol{P}(q^{-1})$ for the noise signal $\mathbf{n}(t+d|t)$.

Our second proposed method, referred to as *Method 2*, is less computationally demanding than *Method 1*. The controller $\mathcal{R}(q^{-1})$ is calculated offline. Only information about the predictability of the feedforward noise is used during the controller design stage. Therefore, $d > 0$ (if the noise is predictable) and $\boldsymbol{F}(q^{-1}) = \boldsymbol{I}$ are used in the diophantine equation (9). During simulation, the simulated time is divided into batches and $\hat{\boldsymbol{F}}(q^{-1})$ is estimated in the same way as in *Method 1*.

The use of a time advance $d > 0$ requires prediction of the feedforward signal, which is illustrated in the block diagram in Figure 3, where the time advance block q^d from Figure 1 has been replaced with a prediction block $\boldsymbol{P}(q^{-1})$. This is a predictor for $\hat{\mathbf{n}}(t+d|t)$ based on the estimate $\hat{\boldsymbol{F}}(q^{-1})$ of the AR noise statistics. The MSE-optimal d-step predictor is used, see e.g. Chapter 12 in (10).

This method will not take full advantage of the knowledge obtained about the feedforward noise signal $\mathbf{n}(t)$ through the estimation of $\hat{\boldsymbol{F}}(q^{-1})$. In order to reduce the computational burden, the repeated solution of the Diophantine equation (9) is in this method interchanged with the calculation of the d-step predictor $\boldsymbol{P}(q^{-1})$, which is much simpler. Since $\hat{\boldsymbol{F}}(q^{-1})$ is diagonal, the calculation of the predictor boils down to L separate systems of equations $\mathbf{Ax} = \mathbf{b}$ where the lower triangular matrix $\mathbf{A}$ has dimensions $(nf+d-1)\times(nf+d-1)$ and $\mathbf{b}$ has dimensions $(nf+d-1)\times 1$. This is readily solved using forward substitution.

4. EXPERIMENTS

Simulations have been performed to evaluate the performance of the proposed methods for adaptation to nonstationary noise statistics. In the simulations, impulse responses measured in a room with dimensions $4.6\times 6\times 2.6$ m were used for the noise path $\boldsymbol{D}(q^{-1})$ and the control path $\boldsymbol{B}(q^{-1})$. These models are used in the controller design, and are in these simulation experiments assumed to be exactly known. The experimental setup for measuring the impulse responses is shown in Figure 4, with 16 loudspeakers placed at different heights around a livingroom sofa. The heights of the different loudspeakers are listed in Table 1. Of the loudspeakers, 14 are used as midrange loudspeakers and the remaining two are subwoofers, marked gray in Figure 4. Using two microphones, the impulse responses from each loudspeaker to 16 measurement positions at ear height above the sofa were measured using swept sinusoids with a sampling frequency of 44.1 kHz. High order FIR models were used in the identification process. The impulse responses were subsampled with a factor 10 to ease the computational burden, leaving a new sampling frequency of 4.41 kHz. The temporal Nyquist frequency for the system is thus 2.2 kHz. However, the spacing of the measurement positions, $d_m = 0.1$ m, gives a spatial Nyquist frequency $f_N = c/2d_m = 344/0.2 = 1720$ Hz. Although lower than the temporal Nyquist frequency, 1720 Hz is well above the frequencies of interest for ANC purposes.

Loudspeaker number 2, marked dark gray in Figure 4, is chosen to act as noise source, and the noise model

[1]The covariance method is e.g. implemented in Matlab's function arcov.m

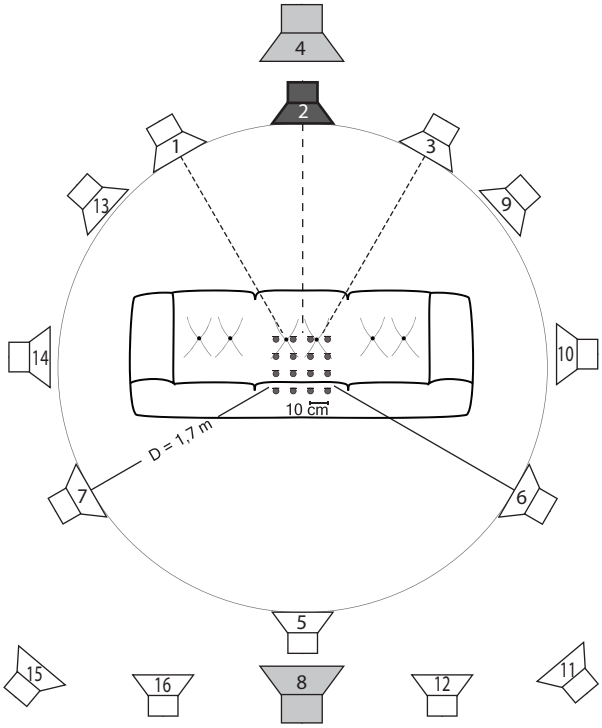

Figure 4 – The experimental setup, consisting of 16 loudspeakers set up around a livingroom sofa over which there are 16 measurement positions forming a 0.3×0.3 m target area for ANC. The loudspeakers that are marked light gray are subwoofers while the rest are used as midrange loudspeakers. The noise source is chosen to be loudspeaker number 2, which is marked dark gray.

is designed as described in Section 3.1 to have properties similar to that of an engine that revs up rather quickly from 2000 rpm to 5000 rpm during 2 seconds. This corresponds to an initial frequency of 66.7 Hz for the first engine order and 133.3 Hz for the second order. These frequencies then increase to 166.7 Hz and 333.3 Hz respectively as the engine speed goes from 2000 rpm to 5000 rpm. The frequency responses of the AR noise model (10) with these specifications for the first and last sample are shown in Figure 5.

Results are presented here for four different simulations:

1. The nonadaptive controller (7) described in Section 2.1 has been used with $\boldsymbol{F} = \boldsymbol{I}$ and $d = 0$ samples in the Diophantine equation (9), i.e. no knowledge of the feedforward signal or its predictability is assumed. This serves as a base-line for the later simulations because it shows what can be achieved with no information about the noise to be cancelled, and will be called *Base Method* below.
2. A time advance $d = 4$ samples is included in (9). Based on the noise statistics at the start of the simulation, an estimate $\hat{\boldsymbol{F}}(q^{-1})$ is calculated. The estimate is used to find a predictor $\boldsymbol{P}(q^{-1})$ for $\hat{\mathbf{n}}(t+d|t)$, and is then kept constant throughout the simulation. This means that the estimate will become more and more outdated as the simulation progresses.

Table 1 – The heights of loudspeakers set up around a living room sofa according to Figure 4.

Speaker number	Height [m]	Speaker Number	Height [m]
1	1.15	9	1.75
2	1.15	10	1.45
3	1.15	11	1.8
4	0.4	12	1.15
5	1.95	13	1.75
6	1.25	14	1.45
7	1.25	15	1.8
8	0.4	16	1.25

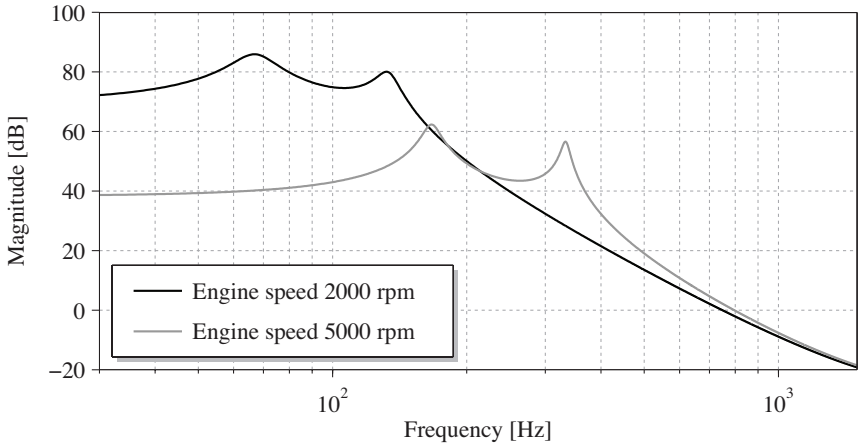

Figure 5 – The initial (black curve) and final (gray curve) frequency responses of the feedforward noise model $\boldsymbol{F}^{-1}(q^{-1})$.

3. The proposed *Method 1* is implemented as described in Section 3.2. The estimate $\hat{\boldsymbol{F}}(q^{-1})$ is updated and the Diophantine equation (9) is solved 10 times per second using $d = 0$ and $\boldsymbol{F} = \hat{\boldsymbol{F}}$, giving a new updated $\boldsymbol{Q}(q^{-1})$ which is used in the controller.
4. The proposed *Method 2* is implemented as described in Section 3.3 with a prediction horizon $d = 4$ samples. This choice of prediction horizon gives the best performance for this method, for the evaluated feedforward signal $\mathbf{n}(t)$. The estimate $\hat{\boldsymbol{F}}(q^{-1})$ and predictor $\boldsymbol{P}(q^{-1})$ are updated 10 times per second, with the estimate for each time batch being based on the feedforward noise signal $\mathbf{n}(t)$ from the previous time batch.

It is worth to note here that the controller used for case 2) and 4) is the same, the only difference between the two cases is that the predictor for the feedforward signal, $\hat{\mathbf{n}}(t+d|t)$ is updated 10 times per second in case 4), as compared to case 2) when it is kept constant. Having set the batch time to 1/10 seconds means that there will be 220 samples in each batch, with the 4.41 kHz sample rate.

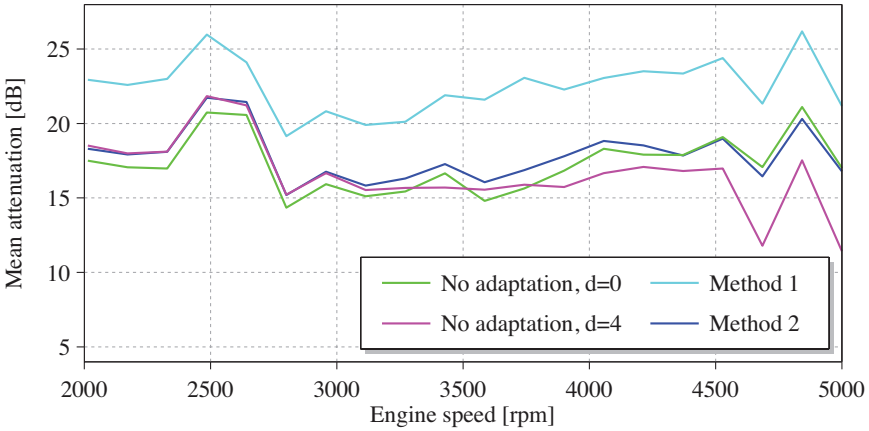

Figure 6 – Mean attenuation from the four simulations plotted in dB against engine speed.

Figure 6 shows the results from the simulations. In the figure, the mean attenuation for the respective case is plotted in dB against rpm. These values are retrieved for each time batch as the mean value over all $M = 16$ measurement positions of the individual attenuations, calculated as

$$\text{Attenuation}_m = -20\log_{10}\left(\frac{||\boldsymbol{\varepsilon}_m(t)||}{||\mathbf{z}_m(t)||}\right), \tag{12}$$

where $\mathbf{z}_m(t)$ and $\boldsymbol{\varepsilon}_m(t)$ are the uncontrolled and controlled time series within each batch for measurement position m. It is obvious from Figure 6 that *Method 1* outperforms the other methods by almost 5 dB throughout. The case with no adaptation but an estimation of the initial noise statistics, plotted in the figure as the magenta line, has approximately 1 dB better performance than *Base Method* initially but the attenuation quickly starts to decline, as expected. Since the estimate is never updated, as the poles of the AR noise model moves away

the prediction of the feedforward signal will degrade. Had the poles been placed closer to the unit circle, the degradation would have been faster.

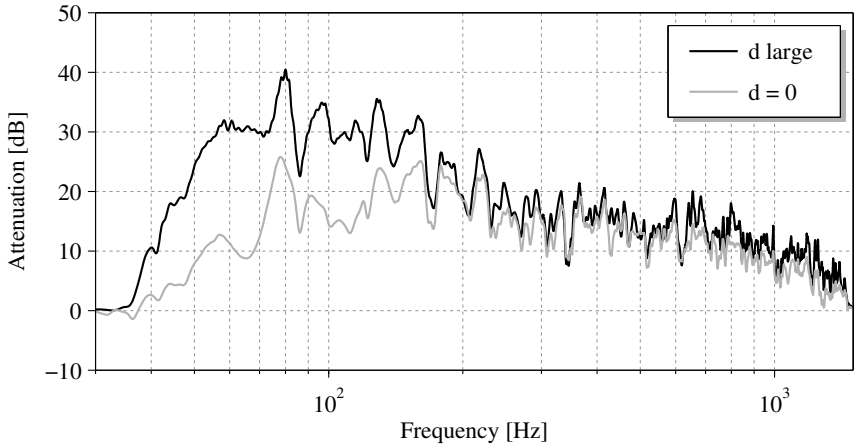

Figure 7 – Theoretical attenuation curves from using a controller with no information of the noise statistics and no time advance d (bottom curve), and a large time advance d, demanding prediction of the feedforward signal (top curve).

When it comes to the performance of *Method 2*, it shows no clear advantage over the *Base method*. Initially *Method 2* shows about 1 dB higher attenuation than *Base method*. However, as the simulation goes on, this small advantage of *Method 2* shrinks. This result is in line with the discussion in (9), where it was shown that a higher time advance d gives rise to a higher achievable attenuation mainly in lower frequencies. This can be illustrated by comparing the theoretical attenuation curves shown in Figure 7. These are the resulting theoretical attenuations for a controller implemented with $\boldsymbol{F}(q^{-1}) = I$ and a very large d in eq. (9), and a controller implemented with $\boldsymbol{F}(q^{-1}) = I$ and $d = 0$ samples in eq. (9). The upper curve shows the attenuations that could be achieved for the system if the feedforward signal could be perfectly predictable arbitrarily far into the future. The lower curve shows the attenuations that could be achieved if no prediction is attempted. Above 250 Hz these curves overlap, meaning that for this system setup, the possibility to predict the feedforward signal will not provide any extra attenuation, as is indeed the case in Figure 6 for higher RPM values. Furthermore, the selected prediction horizon $d = 4$ samples is fairly low. It might not be expected to give a very high gain in attenuation for any frequency range compared to not using any prediction as in *Base method*. Even so, it is of interest to rule out bad modelling as a cause for the lack of improvement, particularly for frequencies below 250 Hz.

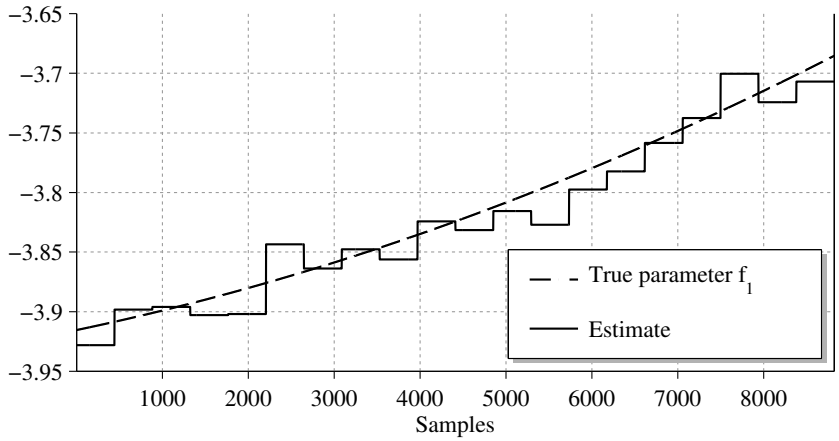

Figure 8 – The true parameter $f_1(t)$ from $\boldsymbol{F}(q^{-1},t)$ and its estimate based on the previous time batch, updated 20 times per second.

Figure 8 shows how the parameter $f_1(t)$ of $\boldsymbol{F}(q^{-1},t)$ in eq. (10) varies over time, together with the estimate for eatch time batch. It is apparent that the estimate lags behind due to the parameter drift. In order to make sure that it is not bad prediction of $\hat{\mathbf{n}}(t+d|t)$ because of bad modelling of $\hat{\boldsymbol{F}}(q^{-1})$ that is responsible for the

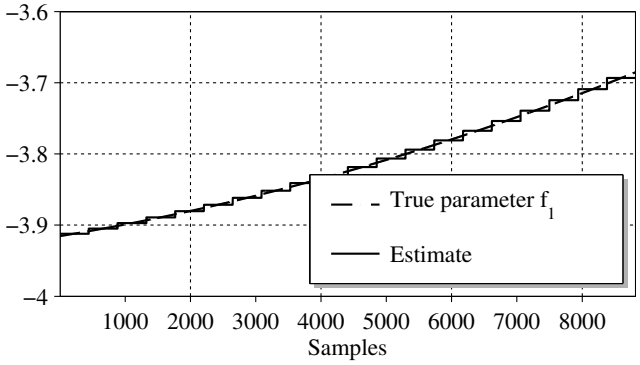

Figure 9 – The true parameter $f_1(t)$ along with the replaced estimate for $f_1(t)$

lack of improvement for *Method 2* over *Base method*, a new simulation is made. This time, the estimate $\hat{\boldsymbol{F}}(q^{-1})$ is replaced with the true parameter value in the middle of each batch, as illustrated in Figure 9. The result from the new simulation is plotted in Figure 10 together with the result from the *Base method* and *Method 1*. There is no noticeable difference between these results and the one in Figure 6 from the first simulation. This indicates that poor modelling is not to blame for the lack of improvement.

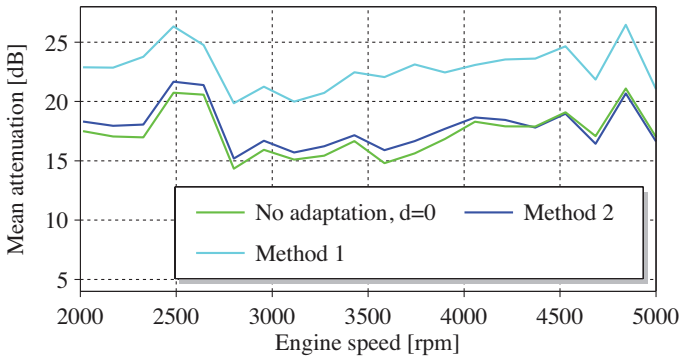

Figure 10 – Results from simulation with the estimate $\hat{\boldsymbol{F}}(q^{-1})$ replaced by the true parameter value at the middle of each time batch.

5. CONCLUSION

In this work, two methods for incorporating adaptation to non-stationary feedforward noise statistics have been proposed and evaluated. The two methods have been compared to a *Base method* that only utilizes knowledge about the noise path and the control path and uses no information about the statistics of the noise, and a variant that uses a fixed estimate of the noise statistics. The latter variant shows the danger of using controllers calculated offline without taking into consideration that conditions change, with deteriorating results as the AR noise model moves away from its initial state.

The more computationally demanding *Method 1*, which involves solving the Diophantine equation (9) repeatedly, has shown to be a promising approach with around 5 dB higher attenuation than *Base method* throughout the simulation, which covers frequencies up to 333.3 Hz. If the noise statistics change slowly enough to allow the time required for updating the controller, then this method is clearly the best alternative of the ones evaluated here.

Method 2, thought as a less computationally demanding alternative to *Method 1* does not show much promise. For the prediction horizon used in the simulation, only around 1 dB higher attenuation is achieved compared to *Base method*, and this only for the low frequencies in the beginning of the simulation. For this method to be worthwhile, longer prediction horizons are needed. However, longer prediction horizons mean higher prediction errors which will counteract any given gain in attenuation. This method might therefore only be of practical use in a situation with extremely narrowband noise signals, that are easily predictable with large prediction horizons.

ACKNOWLEDGEMENTS

This research has been supported by the Swedish Research Counsil under contract 90552701 and by Dirac Research AB. The authors greatfully acknowledge the support from the Knut and Alice Wallenberg foundation (Dnr. KAW 2006.0152) which provided funding for acoustic measurement equipment.

REFERENCES

1. Berthilsson S, Barkefors A, Sternad M. MIMO design of Active Noise Controllers for car interiors: Extending the silenced region at higher frequencies. In: American Control Conference (ACC); 2012. p. 6140–6147.

2. Barkefors A, Berthilsson S, Sternad M. Extending the area silenced by active noise control using multiple loudspeakers. In: Acoustics, Speech and Signal Processing (ICASSP), 2012 IEEE International Conference on; 2012. p. 325–328.

3. Elliott SJ, Nelson PA. Multichannel active sound control using adaptive filtering. In: IEEE International Conference on Acoustics, Speech and Signal Processing ICASSP-88; 1988. p. 2590–2593 vol.5.

4. Sutton TJ, Elliott SJ, McDonald AM, Saunders TJ. Active control of road noise inside vehicles. Noise Control Engineering Journal. 1994 July;42:137–147.

5. Niedzwiecki M, Meller M. A New Approach to Active Noise and Vibration Control-Part I: The Known Frequency Case. IEEE Transactions on Signal Processing. 2009 Sep;57(9):3373–3386.

6. Niedzwiecki M, Meller M. A New Approach to Active Noise and Vibration Control-Part II: The Unknown Frequency Case. IEEE Transactions on Signal Processing. 2009 Sep;57(9):3387–3398.

7. Barkefors A, Sternad M, Brännmark LJ. Design and analysis of linear quadratic gaussian feedforward controllers for active noise control. Accepted for publication;.

8. Hunt KJ, editor. Polynomial Methods in Optimal Control and Filtering. London, UK: Peter Peregrinus; 1993.

9. Barkefors A, Berthilsson S, Sternad M. An investigation of a theoretical tool for predicting performance of an active noise control system. In: International Congress on Sound and Vibration; 2012. .

10. Åström KJ, Wittenmark B. Computer-Controlled Systems: Theory and Design. Upper Saddle River, NJ: Prentice-Hall; 1997.